Analysis of free vibration problems with the Element-Free Galerkin method

Carlos M. Tiago, Vitor M. A. Leitão*
Universidade Técnica de Lisboa, Instituto Superior Técnico
Av. Rovisco Pais, 1049-001 Lisboa, Portugal
e-mail:carlos.tiago@civil.ist.utl.pt, vitor@civil.ist.utl.pt

Abstract

The Element-Free Galerkin (EFG) method is used for the analysis of free vibrations in beams and plates. The associated eigenvalue problem is obtained from a modified Lagrangian functional which provides a suitable constrained Galerkin weak form. In this way the kinematic boundary conditions are included through the introduction of Lagrange multipliers. Numerical tests are conducted on beams, plane states and thin plate bending plate. The effect of varying parameters such as the basis, the number and position of the nodes is assessed.

1 Introduction

For several types of continuum mechanics problems, namely crack propagation, shape optimization, contact, the mesh is an issue in itself: it may be difficult to devise an appropriate mesh due to geometry complexity and/or the solution process may require frequent remeshing. The time taken in creating the mesh (or remeshing) is often several times more than the time needed to form and solve the system of equations. To avoid or reduce the mesh related difficulties, several alternative methods, commonly known as meshless methods [4], have been proposed: the Smoothed Particle Hydrodynamics (SPH) method, the Diffuse Element Method, the Reproducing Kernel Particle Method, the Element–Free Galerkin (EFG) method [5], the *hp*-Clouds Method and the Partition of Unity Finite Element Method, among others.

Meshless methods, in its various approaches, have been applied to a series of engineering problems. The eigenvalue analysis using meshless methods was addressed before by, among others:

- Nagashima [12] used the Node-By-Node Meshless (NBNM) method to analise two dimensional problems;
- the authors [14] used Radial Basis Functions and a collocation approach to analise several unidimensional solid mechanics problems;
- Liu *et al* [11] used the EFG for the analysis of shells;
- Liu [10] used the Meshless Local Petrov-Galerking (MLPG) to analise two dimensional elasticity problems, the EFG to analise thin and thick plates and the Local Point Interpolation Method (LPIM) for beams;

Application of the EFG method to the study of free vibrations in beams and plates is the subject of the present work. Unlike the referred above works, no singular value decomposition is applied to the eigenvalue problem obtained.

The performance of the approach is shown by several numerical 1D and 2D tests.

2 MLS approximations functions

MLS functions were developed, among others, by Lancaster and Salkauskas [9] to approximate curves and surfaces.

Consider a domain, Ω, containing a given set of scattered nodes $\mathbf{x}_i (1 \leq i \leq n)$. Over this set a continuous function, u, assumes the values $\widehat{u}_i$. The MLS approximation of u over Ω, $\widetilde{u}(\mathbf{x})$, is given by:

$$\widetilde{u}(\mathbf{x}) = \sum_{i=1}^{m} p_i(\mathbf{x})\alpha_i(\mathbf{x}) = \mathbf{p}^T(\mathbf{x})\boldsymbol{\alpha}(\mathbf{x}) \tag{1}$$

where $\mathbf{p}(\mathbf{x})$ is a linearly independent basis of m functions,

$$\mathbf{p}^T(x) = \left[\begin{array}{cccc} p_1(\mathbf{x}) & p_2(\mathbf{x}) & \ldots & p_m(\mathbf{x}) \end{array} \right]$$

and $\boldsymbol{\alpha}(x)$ collects the undetermined parameters of the approximation,

$$\boldsymbol{\alpha}^T(\mathbf{x}) = \left[\begin{array}{cccc} \alpha_0(\mathbf{x}) & \alpha_1(\mathbf{x}) & \alpha_2(\mathbf{x}) & \ldots & \alpha_m(\mathbf{x}) \end{array} \right]$$

where each term is a function of the position $\mathbf{x} \in \Omega$.

The parameters $\boldsymbol{\alpha}(\mathbf{x})$ are found at any $\mathbf{x}$ point by minimizing the following weighted least squares discrete L_2 error norm:

$$J(\mathbf{x}) = \sum_{i=1}^{n(\mathbf{x})} w_i(\mathbf{x}-\mathbf{x}_i) \left[\widetilde{u}(\mathbf{x}_i) - \widehat{U}_i\right]^2 = \sum_{i=1}^{n(\mathbf{x})} w_i(\mathbf{x}-\mathbf{x}_i) \left[\mathbf{p}^T(\mathbf{x}_i)\boldsymbol{\alpha}(\mathbf{x}) - \widehat{U}_i\right]^2 \tag{2}$$

where $w_i(\mathbf{x}-\mathbf{x}_i)$ is a weighting function which is nonzero on the influence domain of the node x_i, thus generating a local approximation and sparse matrices.

Only the x_i nodes whose influence domains contain the x point will appear in the sum (2). The dimension of the influence domain of each node and the choice of the weighting function are decisive parameters for the approximation by MLS.

Minimizing $J(x)$ in order to the unknown parameters $\boldsymbol{\alpha}(x)$ results in

$$\boldsymbol{\alpha}(x) = \mathbf{A}^{-1}(x)\mathbf{B}(x)\mathbf{U} \tag{3}$$

where

$$\mathbf{B} = \left[\begin{array}{cccc} w_1(x-x_1)\mathbf{p}(x_1) & w_2(x-x_2)\mathbf{p}(x_2) & \ldots & w_n(x-x_n)\mathbf{p}(x_n) \end{array} \right], \tag{4}$$

$$\mathbf{A} = \sum_{i=1}^{n(x)} w_i(x-x_i)\mathbf{p}^T(x_i)\mathbf{p}(x_i) \qquad \text{and} \qquad \mathbf{U}^T = \left[\begin{array}{cccc} U_1 & U_2 & \ldots & U_n \end{array} \right]. \tag{5}$$

Substituting the result (3) for $\boldsymbol{\alpha}(x)$ in the initial approximation (1), this expression can be written in the usual form

$$\widetilde{u}(x) = \sum_{i=1}^{n} \phi_i(x) U_i = \boldsymbol{\Phi}(x)\mathbf{U} \tag{6}$$

where

$$\phi_i(x) = \sum_{j=1}^{m} p_j(x) \left(\mathbf{A}^{-1}(x)\mathbf{B}(x)\right)_{j\,i} = \mathbf{p}^T\mathbf{A}^{-1}\mathbf{B}_i,$$

$$\boldsymbol{\Phi}(x) = \left[\begin{array}{cccc} \phi_1(x) & \phi_2(x) & \ldots & \phi_n(x) \end{array} \right].$$

3 The eigenvalue problem for solid mechanics

In this section the eigenvalue problem for two dimensional elasticity problems is addressed. The generalization for thin beams and plates, presented in the numerical examples, is straightforward. The resulting expressions are the same and only the definitions of the generalized stresses, $\boldsymbol{\sigma}$, generalized strains, $\boldsymbol{\epsilon}$, generalized displacements $\mathbf{u}$, generalized accelerations $\ddot{\mathbf{u}}$, generalized elasticity operator, $\mathbf{D}$, and differential operator, $\mathbf{L}$, have to be changed.

Let Ω be a open set with piecewise smooth boundary Γ. The boundary can be decomposed in the static part, Γ_t, and the kinematic part, Γ_u, thus $\Gamma = \overline{\Gamma_t \cup \Gamma_u}$, $\Gamma_t \cap \Gamma_u = \emptyset$ and $\overline{\Omega} = \Omega \cup \Gamma$.

The equilibrium equations, in the absence of body forces, are

$$\mathbf{L}^T \boldsymbol{\sigma} = \rho \ddot{\mathbf{u}} \tag{7}$$

where

$$\boldsymbol{\sigma} = \left\{ \begin{array}{c} \sigma_{xx} \\ \sigma_{yy} \\ \sigma_{xy} \end{array} \right\}, \quad \mathbf{L} = \left[\begin{array}{cc} \frac{\partial}{\partial x} & 0 \\ 0 & \frac{\partial}{\partial y} \\ \frac{\partial}{\partial y} & \frac{\partial}{\partial x} \end{array} \right] \quad \text{and} \quad \ddot{\mathbf{u}} = \left\{ \begin{array}{c} \ddot{u} \\ \ddot{v} \end{array} \right\}.$$

The compatibility requires

$$\boldsymbol{\epsilon} = \mathbf{L}\mathbf{u} \tag{8}$$

where $\boldsymbol{\epsilon}^T = \{\epsilon_{xx} \quad \epsilon_{yy} \quad \epsilon_{xy}\}$ and $\mathbf{u}^T = \left\{ \begin{array}{cc} u & v \end{array} \right\}$.

The constitutive equations are given by

$$\boldsymbol{\sigma} = \mathbf{D}\boldsymbol{\epsilon} \tag{9}$$

where, assuming a plane stress state,

$$\mathbf{D} = \frac{E}{1-\nu^2} \left[\begin{array}{ccc} 1 & \nu & 0 \\ \nu & 1 & 0 \\ 0 & 0 & \frac{1-\nu}{2} \end{array} \right]$$

and E is the elasticity modulus and ν is the Poisson's ratio.

The (homogeneous) boundary conditions are given by

$$\mathbf{u} = \mathbf{0} \tag{10a}$$

$$\mathbf{N}\boldsymbol{\sigma} = \mathbf{0} \tag{10b}$$

where $\mathbf{N}$ is the matrix of the unit outward normal components associated with the differential operator $\mathbf{L}$.

4 Variational form of the eigenvalue problem

The variational form of the eigenvalue problem can be derived directly from the Hamilton's Principle:

$$\delta \int_{t_1}^{t_2} L \, \mathrm{d}t = 0 \tag{11}$$

where L is the Lagrangian function of the system, leading to the generalization of the well known principle of virtual work for an undamped vibration system:

$$\int_\Omega \delta\boldsymbol{\epsilon}^T \boldsymbol{\sigma} \mathrm{d}\Omega + \int_\Omega \rho \delta \mathbf{u}^T \ddot{\mathbf{u}} \mathrm{d}\Omega = 0. \tag{12}$$

(Recall that it is assumed that no body forces and prescribed tractions are applied).

In equation (12) it is assumed that the approximation of the displacement field meets the kinematic boundary conditions, but the MLS approximation (1) does not satisfy the Kronecker delta criterion: $\Phi_I(x_J) \neq \delta_{IJ}$. One possible way to include such restrictions is the use of a generalized variational form as presented by Washizu [15] and Liu [10]. Using a modified Lagrangian in (11) which includes the kinematic boundary conditions through the use of additional variables, results in the following variational form:

$$\int_\Omega \delta\boldsymbol{\epsilon}^T\boldsymbol{\sigma}\mathrm{d}\Omega - \int_{\Gamma_u} \delta\boldsymbol{\lambda}^T\mathbf{u}\mathrm{d}\Gamma_u - \int_{\Gamma_u} \boldsymbol{\lambda}^T\delta\mathbf{u}\mathrm{d}\Gamma_u + \int_\Omega \rho\delta\mathbf{u}^T\ddot{\mathbf{u}}\mathrm{d}\Omega = 0. \tag{13}$$

The additional variables are the Lagrange multipliers $\boldsymbol{\lambda}^T = \left\{ \begin{array}{cc} \lambda_u & \lambda_v \end{array} \right\}$.

For the free vibration problem the system responds in harmonic motion and the separation of variables technique can be used. The displacement field takes then the following form:

$$\mathbf{u}(\mathbf{x}, t) = \mathbf{u}(\mathbf{x})\sin(\omega t + \varphi) \tag{14}$$

where ω is the circular frequency of the system and φ is the phase angle. Substituting (14) in (13) and using (7), (8) and (9) it follows

$$\int_\Omega \delta(\mathbf{L}\,\mathbf{u})^T\mathbf{D}\,(\mathbf{L}\,\mathbf{u})\mathrm{d}\Omega - \int_{\Gamma_u} \delta\boldsymbol{\lambda}^T\mathbf{u}\mathrm{d}\Gamma_u - \int_{\Gamma_u} \boldsymbol{\lambda}^T\delta\mathbf{u}\mathrm{d}\Gamma_u + \int_\Omega \rho\omega^2\delta\mathbf{u}^T\mathbf{u}\mathrm{d}\Omega = 0. \tag{15}$$

5 Discrete equations

The expression of the MLS approximation (6) for a two dimensional elasticity problem is redefined as follows:

$$\tilde{\mathbf{u}} = \boldsymbol{\Phi}\,\mathbf{U} \tag{16}$$

where

$$\tilde{\mathbf{u}} = \left\{ \begin{array}{c} \tilde{u} \\ \tilde{v} \end{array} \right\}, \boldsymbol{\Phi} = \left[\begin{array}{ccccc} \phi_1 & 0 & \dots & \phi_n & 0 \\ 0 & \phi_1 & \dots & 0 & \phi_n \end{array} \right] \text{ and } \mathbf{U}^T = \left\{ \begin{array}{cccccc} U_1 & V_1 & \dots & U_n & V_n \end{array} \right\}.$$

Taking variations over (16) results in

$$\delta\tilde{\mathbf{u}} = \boldsymbol{\Phi}\,\delta\mathbf{U}. \tag{17}$$

The discretization of the Lagrange multipliers is made by resorting to the traditional Lagrange interpolants of the conventional Finite Element Method (FEM):

$$\boldsymbol{\lambda} = \mathbf{N}\boldsymbol{\Lambda} \tag{18}$$

where

$$\mathbf{N} = \left\{ \begin{array}{ccccc} N_1 & 0 & \dots & N_{n_\lambda} & 0 \\ 0 & N_1 & \dots & 0 & N_{n_\lambda} \end{array} \right\} \text{ and } \boldsymbol{\Lambda}^T = \left\{ \begin{array}{cccccc} \lambda_{u_1} & \lambda_{v_1} & \dots & \lambda_{u_{n_\lambda}} & \lambda_{v_{n_\lambda}} \end{array} \right\}$$

and n_λ is the number of nodes associated with the discrete variables that provide the interpolation for λ.

Taking variations over (18) results in

$$\delta\boldsymbol{\lambda} = \mathbf{N}\delta\boldsymbol{\Lambda}. \tag{19}$$

Using the approximation (16) and (17) for the fields $\mathbf{u}$ and $\delta\mathbf{u}$ and the expressions (18) and (19) on (15), for arbitrary variations of $\delta\mathbf{u}$ and $\delta\boldsymbol{\lambda}$, the discretized form of the eigenvalue problem is given by

$$\left[\begin{array}{cc} \mathbf{K} - \omega^2\mathbf{M} & \mathbf{G} \\ \mathbf{G}^T & \mathbf{0} \end{array} \right] \left\{ \begin{array}{c} \mathbf{U} \\ \boldsymbol{\Lambda} \end{array} \right\} = 0 \tag{20}$$

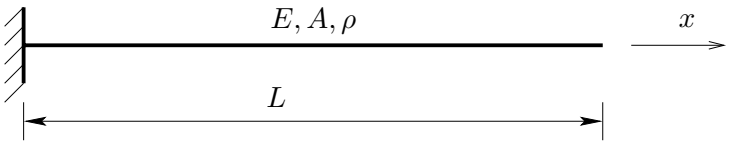

Figure 1: Properties of bar subjected to axial vibration.

where

$$\mathbf{K} = \int_\Omega \mathbf{B}^T\mathbf{D}\mathbf{B}\mathrm{d}\Omega, \quad \mathbf{M} = \int_\Omega \mathbf{\Phi}^T\rho\mathbf{\Phi}\mathrm{d}\Omega \quad \text{and} \quad \mathbf{G} = -\int_{\Gamma_u} \mathbf{\Phi}^T\mathbf{N}\mathrm{d}\Gamma_u.$$

The corresponding eigenvalues of problem (20) are the solutions of

$$\begin{vmatrix} \mathbf{K} - \omega^2\mathbf{M} & \mathbf{G} \\ \mathbf{G}^T & \mathbf{0} \end{vmatrix} = 0. \tag{21}$$

6 Numerical examples

The basis $\mathbf{p}$ used in the examples is given by polynomials: $\mathbf{p}^T = \left\{ \begin{array}{cccc} 1 & x & x^2 & \dots \end{array} \right\}$ for 1D and $\mathbf{p}^T = \left\{ \begin{array}{ccccccccccc} 1 & x & y & x^2 & xy & y^2 & x^3 & x^2y & xy^2 & y^3 & \dots \end{array} \right\}$ for 2D.

The nodes are equally spaced and the background cells for the integrations are defined by the spaces between the nodes. In all examples Gauss-quadrature is used.

The numerical implementation was carried out MATLAB [8] with calls to LAPACK [1] being made to solve the generalized eigenvalue problem (20).

6.1 One-dimensional vibration examples

The distance $d_{m\,i}$ is equal for all nodes and is taken as the minimum distance that makes the matrix $\mathbf{A}$ in expression (3) non-singular at all Gauss points.

The weighting function used is the quartic spline

$$w(x - x_i) = \begin{cases} 1 - 6r^2 + 8r^3 - 3r^4, & \text{if} \quad \|x - x_i\| \le d_{m\,i} \\ 0, & \text{if} \quad \|x - x_i\| > d_{m\,i} \end{cases} \tag{22}$$

where $r = \frac{\|x-x_i\|}{d_{m\,i}}$ and $d_{m\,i}$ is the size of the influence domain.

6.1.1 Axial vibration

Consider the cantilever represented in Figure 1. The exact solution for the vibration circular frequencies and mode shapes [6] is given by

$$w_n = \frac{\pi}{2}(2n-1)\sqrt{\frac{EA}{\rho L^2}}, \qquad \overline{\phi}_n = C\sin\left[\frac{\pi}{2}(2n-1)\frac{x}{L}\right] \qquad n = 1, 2, 3, \dots$$

Figure 2 shows the error in the first ten frequencies obtained for different number of nodes with a linear basis. A five sampling points integration rule was used. A comparison of the first five modes shapes is presented in Figure 3 for the ten node discretization.

Figure 4 shows the error in the first four frequencies obtained with different number of elements in the basis, m. A fifteen sampling points integration rule was used due to the increase of the highest exponent in the basis. Exact solutions would be obtained if sine waves basis were to be used.

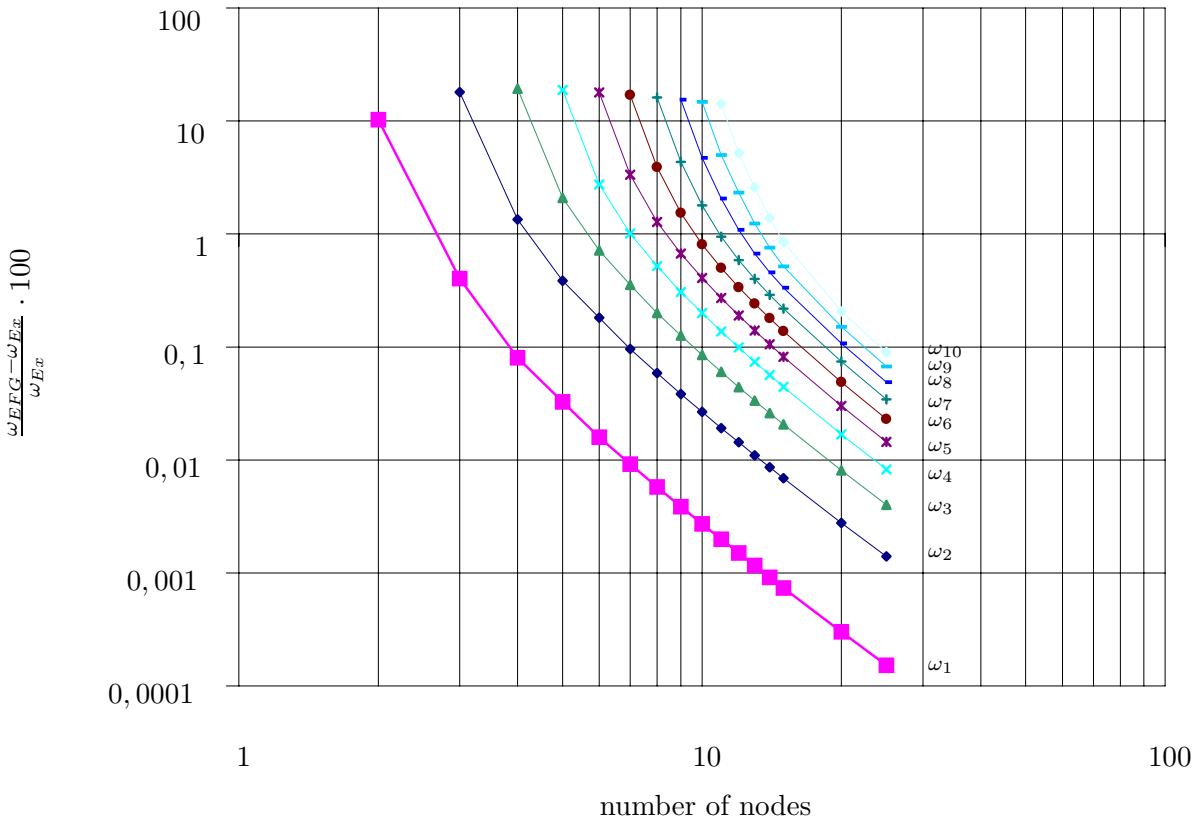

Figure 2: Frequency relative error for bar subjected to axial vibration with a linear basis, $\mathbf{p}^T = \{1 \quad x\}$.

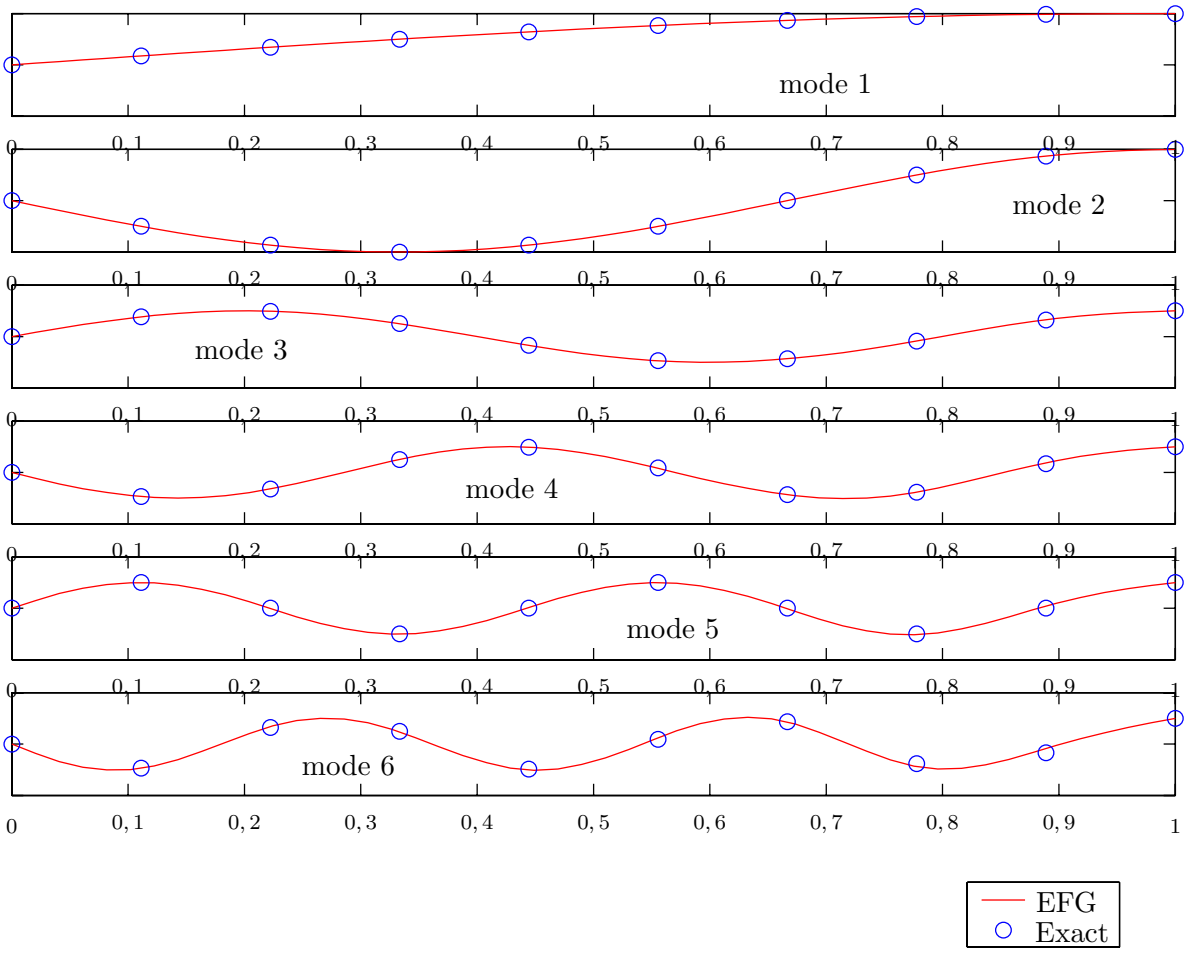

Figure 3: First six vibration mode shapes for bar subjected to axial vibration with linear basis and ten nodes.

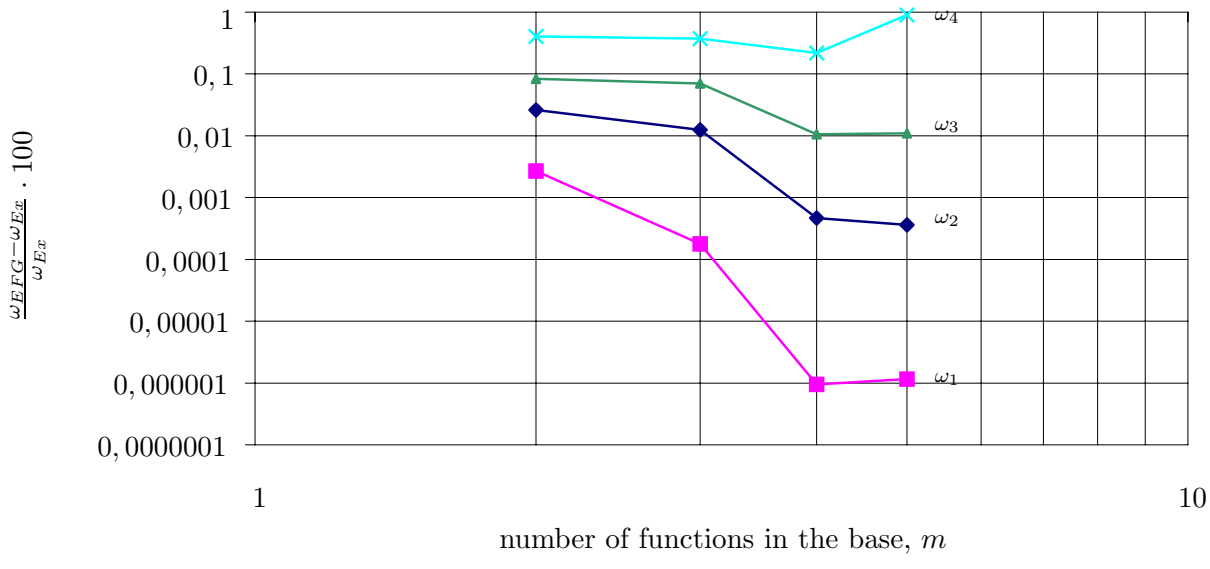

Figure 4: Frequency relative error for bar subjected to axial vibration with ten nodes.

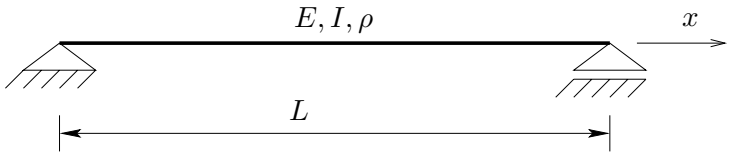

Figure 5: Properties of beam subjected to flexural vibration.

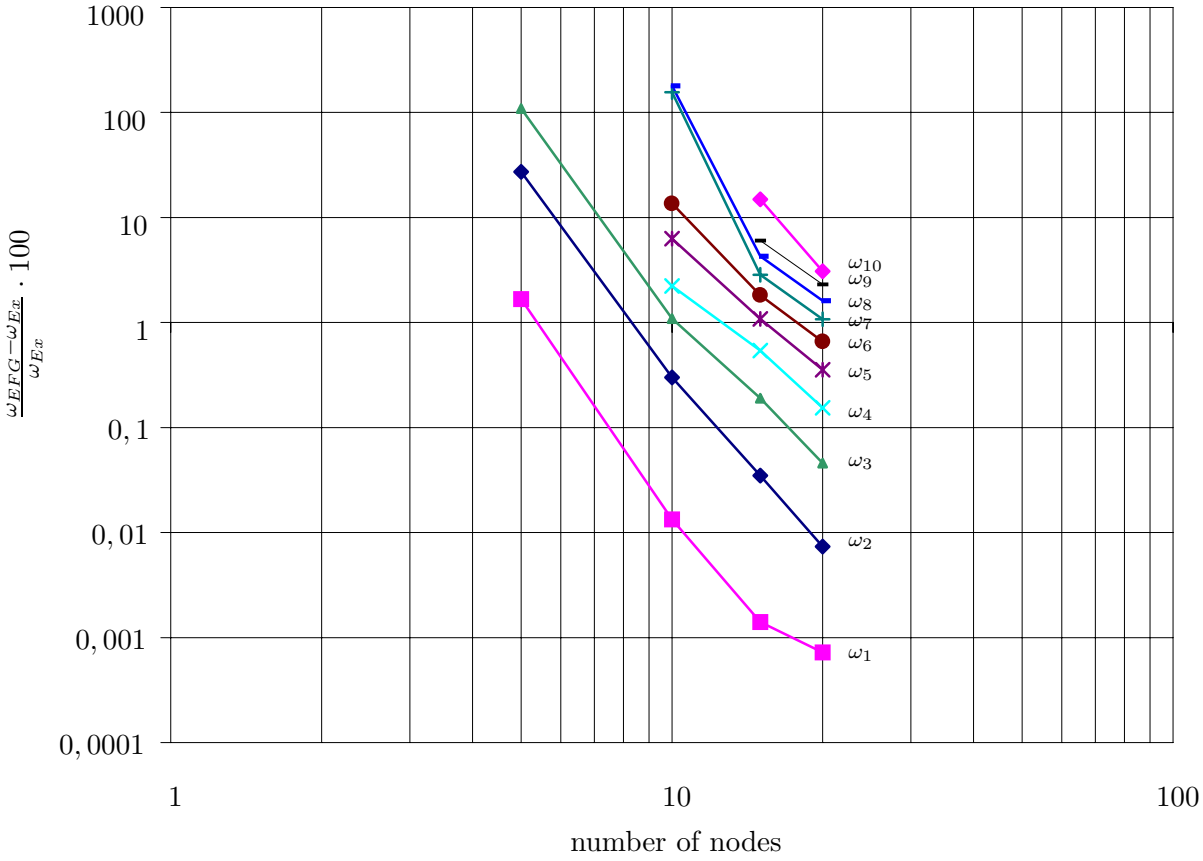

Figure 6: Frequency relative error for bar subjected to flexural vibration with a cubic basis, $\mathbf{p}^T = \{1 \quad x \quad x^2 \quad x^3\}$.

6.1.2 Flexural vibration

Consider the simply supported beam represented in Figure 5. The exact solution for the vibration circular frequencies and mode shapes [6] is given by

$$w_n = n^2\pi^2\sqrt{\frac{EI}{\rho L^4}}, \qquad \overline{\phi}_n = C\sin\left(\frac{n\pi x}{L}\right) \qquad n = 1, 2, 3, \ldots$$

Figure 6 shows the error in the first ten frequencies obtained for different number of nodes with a cubic basis. A ten sampling points integration rule was used.

A comparison of the first five modes shapes is presented in Figure 7 for the fifteen node discretization.

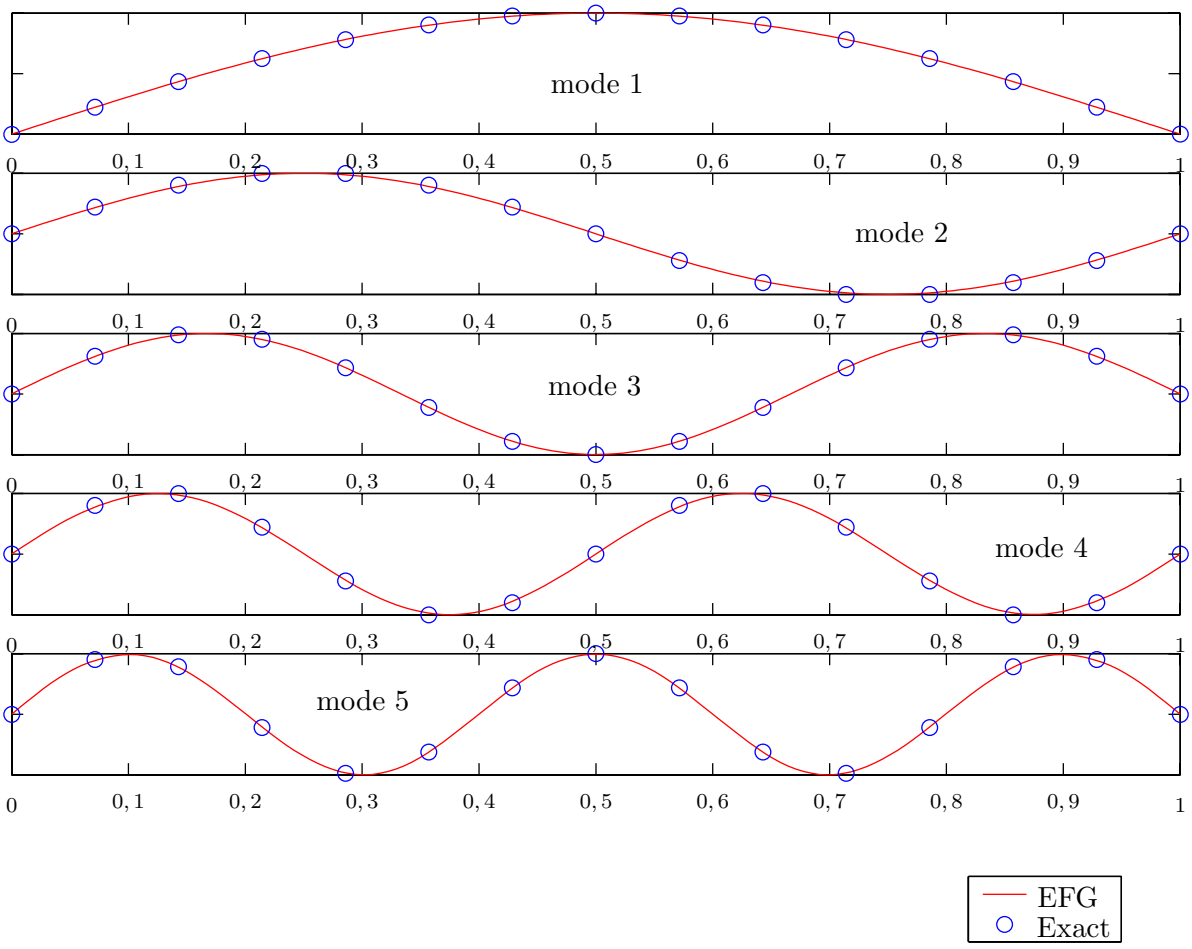

Figure 7: First five vibration modes shapes for beam subjected to flexural vibration with cubic basis and fifteen nodes.

Young's modulus	$E = 2,1 \times 10^4\,\mathrm{kgf/mm^2}$
Poisson's ratio	$\nu = 0,3$
Mass density	$\rho = 8,0 \times 10^{-10}\,\mathrm{kgf\ s^2/mm^4}$
Thickness	$t = 1\,\mathrm{mm}$
Height	$D = 10\,\mathrm{mm}$
Length	$L = 100\,\mathrm{mm}$

Table 1: Cantilever beam on plane stress properties.

Mode	ADINA	EFG			MLPG	NBNM
	4221 nodes	22 nodes	63 nodes	124 nodes	306 nodes	306 nodes
1	822,13	869,76	824,71	822,57	844,19	824,44
2	4 931,95	5 175,71	4917,67	4 887,02	5070,32	5051,21

Table 2: Plane stress cantilever beam: first two cyclic frequencies [Hz].

6.2 Two-dimensional vibration examples

The weighting function used in this work is [2]

$$w(\mathbf{x}-\mathbf{x}_i) = \begin{cases} \left(1 - \|\mathbf{x}-\mathbf{x}_i\|^2/d_{m\,i}^2\right)^s, & \text{if} \quad \|\mathbf{x}-\mathbf{x}_i\| \le d_{m\,i} \\ 0, & \text{if} \quad \|\mathbf{x}-\mathbf{x}_i\| > d_{m\,i} \end{cases} \tag{23}$$

where $d_{m\,i}$ is the size of the influence domain of the i^{th} node.

Linear Lagrange interpolation functions were used for the matrix $\mathbf{N}$ in the expansions (18) and (19).

6.2.1 Plane state

Consider now a cantilever beam with properties as in Table 1, modelled as a plane stress state. This problem was previously analyzed by Nagashima [12] by the Node-By-Node Meshless method (NBNM) and Liu [10] using the Meshless Local Petrov-Galerkin method (MLPG) [3].

A linear basis was used, $\mathbf{p}^T = \left\{ \begin{array}{ccc} 1 & x & y \end{array} \right\}$ and the size of the influence domain was set equal to three times the distance between nodes (which was equal in both directions). The parameter s in expression (23) was taken equal to 2.

The results obtained for the first two natural frequencies are compared with other solutions in Table 2. The ADINA [7] code was used to generate a solution with 1 000 traditional elements (9 node Lagrangian element) and 4221 nodes.

The solutions with 22, 63 and 124 nodes correspond, respectively, to 1×10, 2×20 and 3×30 divisions of the beam in each direction. A six points quadrature rule in each direction, in each cell, was used.

The first two vibration modes for the solution with 63 nodes are displayed in Figure 8. The background cells and the nodes are also displayed.

6.2.2 Plate bending vibration

Consider a square simply supported thin plate with side length a, thickness h, flexural stiffness $D = \frac{Eh^3}{12(1-\nu^2)}$.

The exact solution for the frequencies, neglecting the rotary inertia, is given by Reddy [13]:

$$\omega_{mn} = \frac{\pi^2}{a^2}\sqrt{\frac{D}{\rho h}}\left(m^2+n^2\right).$$

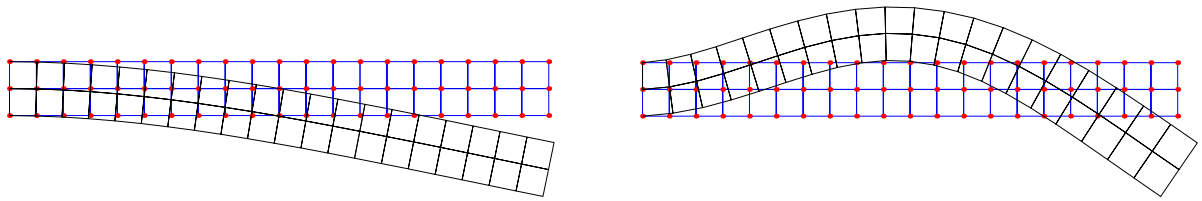

(a) First vibration mode. (b) Second vibration mode.

Figure 8: First two vibration modes of plane stress cantilever beam.

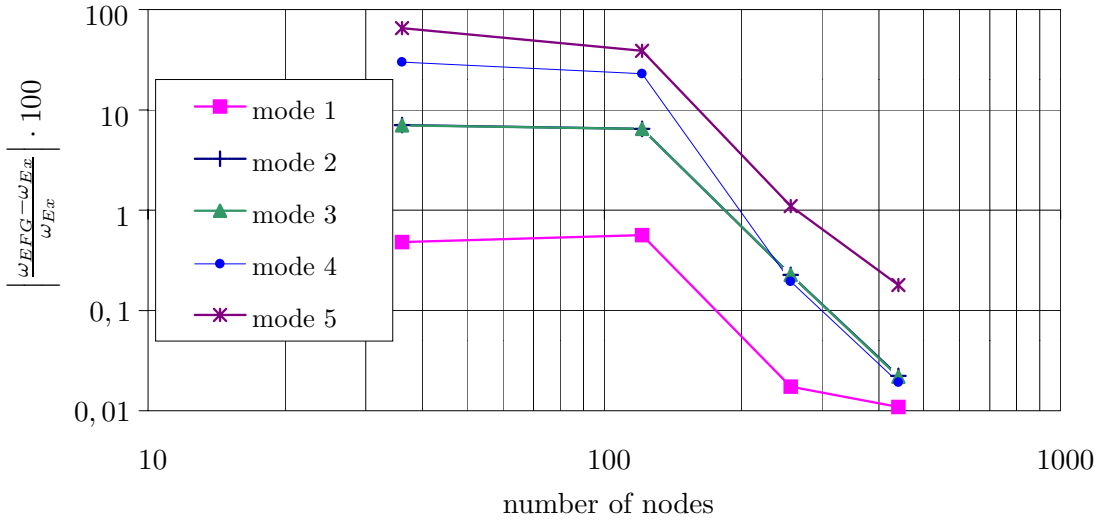

Figure 9: Frequency error for simply supported plate.

A cubic base, $\mathbf{p}^T = \{ 1 \quad x \quad y \quad x^2 \quad xy \quad y^2 \quad x^3 \quad x^2y \quad xy^2 \quad y^3 \}$ was used. The domain of influence is always square and its length is four times the node spacing. The nodes are located at square grid positions corresponding to 5, 10, 15 and 20 divisions of the length of the plate. The parameter s in expression (23) was taken equal to 3. Due to symmetry, the second and third modes have the same frequency, thus the corresponding lines in the figure are nearly identical.

The first four vibration modes are represented in Figures 10, 11, 12 and 13.

7 Conclusions

In this work an implementation of the EFG method for the analysis of one-dimensional and two-dimensional free vibration problems was presented.

The variational statement for the eigenvalue problem is discretized with the use of Lagrange multipliers.

The resultas obtained show the accuracy and the good convergence properties of the technique. Further developments should include the analysis of forced vibrations.

Acknowledgments

This work has been partially supported by FCT through projects "Financiamento Plurianual" and POCTI/33066/ECM/2000.

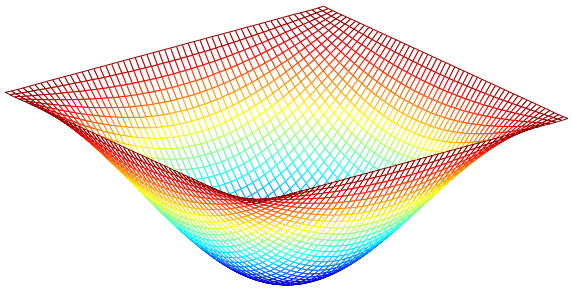

Figure 10: First vibration mode.

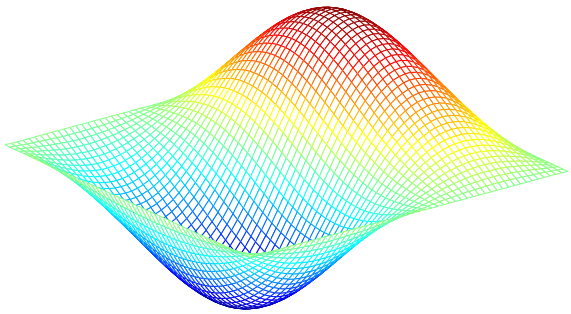

Figure 11: Second vibration mode.

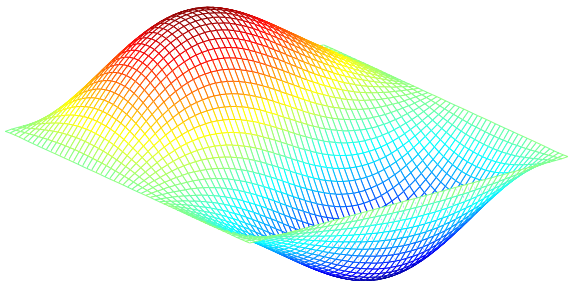

Figure 12: Third vibration mode.

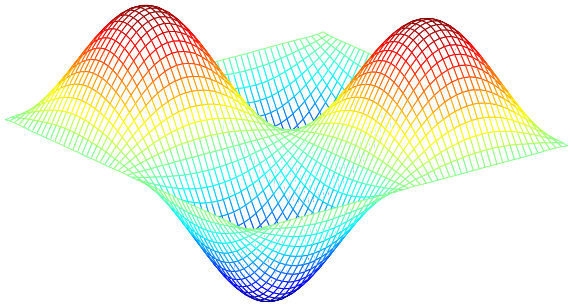

Figure 13: Fourth vibration mode.

References

[1] E. Anderson, Z. Bai, C. Bischof, S. Blackford, J. Demmel, J. Dongarra, J. Du Croz, A. Greenbaum, S. Hammarling, A. McKenney, and D. Sorensen. *LAPACK User's Guide*. Siam, Philadelphia, 1999.

[2] S. N. Atluri, J. Y. Cho, and H.-G. Kim. Analysis of thin beams, using the meshless local Petrov-Galerkin method, with generalized moving least squares interpolations. *Comput. Mech.*, 24:334–347, 1999.

[3] S. N. Atluri and T.-L. Zhu. The meshless local Petrov-Galerkin (MLPG) approach for solving problems in elasto-statics. *Comput. Mech.*, 25:169–179, 2000.

[4] T. Belytschko, Y. Krongauz, D. Organ, M. Fleming, and P. Krysl. Meshless methods: An overview and recent developments. *Comput. Methods Appl. Mech. Engrg.*, 139:3–47, 1996.

[5] T. Belytschko, Y. Lu, and L. Gu. Element-Free Galerkin Methods. *Int. J. Numer. Meth. Engng.*, 37:229–256, 1994.

[6] R. W. Clough and J. Penzien. *Dynamics of Structures*. Mc Graw-Hill International Editions, second edition, 1993.

[7] ADINA R & D Inc. *Theory and Modeling Guide - Volume I: ADINA, Report ARD 02-7*. 2002.

[8] The MathWorks Inc. *MATLAB, The Language of Technical Computing*. Version 6.0, 2000.

[9] P. Lancaster and K. Salkauskas. Surfaces genarated by the moving least squares methods. *Math. Comput.*, 37:141–158, 1981.

[10] G. R. Liu. *Mesh Free Methods: Moving beyond the Finite Element Method*. CRC Press, 2003.

[11] L. Liu, G. R. Liu, and V. B. C. Tan. Element free method for static and free vibration analysis of spatial thin shell structures. *Comput. Methods Appl. Mech. Engrg.*, 191:5923–5942, 2002.

[12] T. Nagashima. Node-by-node meshless approach and its applications to structural analyses. *Int. J. Numer. Meth. Engng.*, 46:341–385, 1999.

[13] J. N. Reddy. *Theory and analysis of elastic plates*. Taylor & Francis, 1999.

[14] C. Tiago and V.M.A. Leitão. Utilização de funções de base radial em problemas unidimensionais de análise estrutural. In J. M. Goicolea, C. Mota Soares, M. Pastor, and G. Bugeda, editors, *Métodos Numéricos en Ingeniería V, CD*. SEMNI, 2002.

[15] K. Washizu. *Variational Methods in Elasticity and Plasticity*. Pergamon Press, second edition, 1975.